Human Molecular Genetics, 2024, Vol. 33, 1, 48–63
https://doi.org/10.1093/hmg/ddad160
Advance access publication date 22 September 2023
Original Article

Higher incidence of embryonic defects in mouse offspring conceived with assisted reproduction from fathers with sperm epimutations

Gurbet Karahan[1,2], Josée Martel[2], Sophia Rahimi[2], Mena Farag[1], Fernando Matias[3], Amanda J. MacFarlane[3,†], Donovan Chan[2], Jacquetta Trasler[1,2,4,5,*]

[1]Department of Human Genetics, McGill University, Montreal, QC, H3A 0C7, Canada
[2]Research Institute of the McGill University Health Centre, Montreal, QC, H4A 3J1, Canada
[3]Nutrition Research Division, Health Canada, Ottawa, ON, K1A 0K9, Canada
[4]Department of Pharmacology and Therapeutics, McGill University, Montreal, QC, H3G 1Y6, Canada
[5]Department of Pediatrics, McGill University Health Centre, Montreal, QC, H4A 3J1, Canada
*Corresponding author. 1001 Décarie Blvd., Glen site of the RI-MUHC, EM0.2236, Montreal, QC H4A 3J1, Canada. Tel: 1-514-934-1934 ext. 25235; E-mail: jacquetta.trasler@mcgill.ca

[†]Present address: Agriculture, Food, and Nutrition Evidence Center, Texas A&M University System, Fort Worth, TX, 76102, USA

Abstract

Assisted reproductive technologies (ART) account for 1–6% of births in developed countries. While most children conceived are healthy, increases in birth and genomic imprinting defects have been reported; such abnormal outcomes have been attributed to underlying parental infertility and/or the ART used. Here, we assessed whether paternal genetic and lifestyle factors, that are associated with male infertility and affect the sperm epigenome, can influence ART outcomes. We examined how paternal factors, haploinsufficiency for *Dnmt3L*, an important co-factor for DNA methylation reactions, and/or diet-induced obesity, in combination with ART (superovulation, *in vitro* fertilization, embryo culture and embryo transfer), could adversely influence embryo development and DNA methylation patterning in mice. While male mice fed high-fat diets (HFD) gained weight and showed perturbed metabolic health, their sperm DNA methylation was minimally affected by the diet. In contrast, *Dnmt3L* haploinsufficiency induced a marked loss of DNA methylation in sperm; notably, regions affected were associated with neurodevelopmental pathways and enriched in young retrotransposons, sequences that can have functional consequences in the next generation. Following ART, placental imprinted gene methylation and growth parameters were impacted by one or both paternal factors. For embryos conceived by natural conception, abnormality rates were similar for WT and *Dnmt3L*$^{+/-}$ fathers. In contrast, paternal *Dnmt3L*$^{+/-}$ genotype, as compared to WT fathers, resulted in a 3-fold increase in the incidence of morphological abnormalities in embryos generated by ART. Together, the results indicate that embryonic morphological and epigenetic defects associated with ART may be exacerbated in offspring conceived by fathers with sperm epimutations.

Keywords: Dnmt3L-haploinsufficiency; assisted reproduction; DNA methylation; sperm epimutations; male infertility

Introduction

Around 15% of couples experience difficulties conceiving, with underlying infertility attributed to the woman, the man, the couple, or unknown causes. Assisted reproductive technologies (ART) are increasingly used to help those struggling with infertility and account for 1–6% of live births in high income countries [1]. Although ART is accepted as a safe method of conception, offspring are at a small but still significant increased risk for birth defects [2]. ART has also been associated with rare genomic imprinting disorders, such as Beckwith-Wiedemann syndrome, where altered DNA methylation has been implicated [3–6]. The cause of the increases in birth and genomic imprinting defects has been attributed to the techniques used in assisted reproduction and/or the underlying parental infertility.

ART typically consists of manipulations such as *in vitro* fertilization (IVF) and intracytoplasmic sperm injection (ICSI), accompanied by superovulation, oocyte retrieval, embryo culture, and embryo transfer. Many of these techniques coincide with important DNA methylation reprogramming windows, including the establishment of female-specific epigenetic patterns in oocytes and global erasure during pre-implantation development [7]. We and others have shown that superovulation can alter oocyte quality and perturb the maintenance of DNA methylation of both maternally and paternally methylated imprinted genes during preimplantation development in mice [8–11]. Furthermore, studies in mice showed that as the number of ART procedures increases, so do the morphological abnormalities and epigenetic perturbations in offspring placentas, indicating that ART-induced epigenetic perturbations may be additive [12]. These and other studies performed in mice, without parental infertility, provide evidence that ART alone is capable of inducing adverse offspring outcomes [12–15]. However, interpretation of human ART studies is more complex, where underlying causes of infertility/subfertility may also play a role [4, 16, 17].

Received: May 31, 2023. **Revised:** August 30, 2023. **Accepted:** September 13, 2023

Maternal factors associated with infertility and their contribution to offspring growth and development have been relatively well studied. Less attention has been focused on male factors associated with infertility and how they may contribute to adverse outcomes, in particular those linked to ART. Sperm not only provide genetic information, but are also important carriers of epigenetic information (DNA methylation, chromatin modifications and small RNAs) that can be influenced by internal (gene defects) and external/environmental factors. These factors may cause epimutations, where altered epigenetic states (e.g. DNA methylation) can occur in the absence of changes in DNA sequence. Such factors have been shown to influence offspring growth and development [18–23]. Controlled mouse studies can therefore help determine the contribution of individual and/or combined paternal factors to birth defects and abnormal health outcomes associated with ART.

Genetic abnormalities in critical genes can have a negative impact on male fertility. Some of these variations can also influence sperm DNA methylation, which can be transmitted to the offspring. DNA methyltransferase 3-like (DNMT3L) is a protein essential for the establishment of DNA methylation patterns in male germ cells. It is a co-factor that interacts with the DNA methylating enzymes, DNMT3A and DNMT3B, to stimulate their activity [24–26]. In humans, *DNMT3L* copy number variations or mutations (SNP) are found in infertile men in some studies [17, 27–29]. The most studied polymorphism examined has been rs7354779, a missense mutation (C/T; frequency ~0.28) that causes an amino acid change in exon 10 (Arg278Gly) [30]. This mutation occurs in the C-terminal, which interacts with the active catalytic methyltransferase domain of DNMT3A and DNMT3B [31, 32]. While other mutations have been examined, their minor allele frequencies have been reported to be <0.01 [30]. In animal models, although *Dnmt3L* knock-out male mice are viable, they are sterile. Their germ cells possess abnormally low levels of DNA methylation, including hypomethylation of paternally methylated imprinted genes and transposable elements [33, 34]. As a paternal effect gene, *Dnmt3L* haploinsufficiency (*Dnmt3L*$^{+/-}$) results in wild-type (WT) progeny demonstrating abnormal phenotypes [35, 36]. Taken together, the mouse and human findings indicate that *Dnmt3L* is a good candidate gene to investigate the effect of sperm DNA methylation perturbations on ART conceived offspring.

In addition to genetic abnormalities, environmental factors may also affect reproductive health and sperm DNA methylation. Obesity is an epidemic that affects approximately 42% of adult males aged >20 in the United States, with 6.9% of men suffering from severe obesity [37]. Being overweight can negatively impact male fertility through several mechanisms, including hypogonadism, impaired spermatogenesis, and lower serum testosterone levels [38]. Additionally, studies in humans and rodents have demonstrated that obesity and high-fat diets (HFD) can affect DNA methylation patterns in male germs cells [20, 39–41] The number of obese men coming to infertility clinics has tripled in the last few decades [42]. Furthermore, obese men undergoing IVF have lower clinical pregnancy and live birth rates [43]. Epidemiological studies provide further support indicating that the father's diet is capable of affecting the offspring's health and well-being [44, 45]. Animal models for obesity, HFD fed male mice or rats, have been used to investigate offspring characteristics. Progeny from HFD-fed fathers have demonstrated several phenotypes, indicating an intergenerational effect of obesity even without the use of ART [40, 46–48].

In this study, using a mouse model, we investigated whether the paternal factors, *Dnmt3L* haploinsufficiency and an obesogenic HFD, alone or together, could affect genome-wide sperm DNA methylation patterns. Additionally, we wanted to examine if these paternal factors, when combined with assisted reproduction, would exacerbate the negative effects of ART on offspring development. We find that, while HFD minimally affected the sperm DNA methylome, *Dnmt3L* haploinsufficiency resulted in genome-wide sperm DNA hypomethylation. Through the use of ART, *Dnmt3L*$^{+/-}$ fathers produced litters with a significantly higher number of abnormal embryos, independent of diet. Here, we provide evidence that a genetic disorder, that results in sperm epimutations, can worsen ART-dependent outcomes in the next generation. We propose that the exacerbation of ART-related adverse embryonic and epigenetic outcomes is due to the combined effects of an abnormal sperm DNA methylome and a suboptimal environment caused by ART used during critical times of epigenetic reprogramming in the embryo.

Materials and methods

Animals

The *Dnmt3L*$^{tm/Bes}$ mouse line was a gift from Timothy Bestor and Deborah Bourc'his [34]; this line was kept on a C57BL/6 background. GFP transgenic mice with the Oct4 proximal promoter driving the expression of GFP were generously provided by Hans Schöler [49] and crossed with *Dnmt3L*$^{+/-}$ or WT males. WT C57BL/6 male mice (6–7 weeks of age) were purchased from Charles River Canada Inc. (QC, Canada) and Hsd:NSA (CF1) females (6–7 weeks of age) were purchased from Envigo (IN, USA) and they were allowed at least one week of acclimation period before start of the diets, breeding, or ART. All animals were housed in a pathogen-free, temperature-controlled room with a 12 h light, 12 h dark cycle and had free access to water and food *ad libitum*. Body weights were measured and recorded each week. All animal work was performed following the Canadian Council on Animal Care guidelines and approved by the Animal Care Committee at the Research Institute of the McGill University Health Centre in Montreal.

Diets

All males (until 8 weeks of age) and CF1 females (throughout the course of the study), were fed Teklad Global 18% Protein Rodent Diet 2018 (Envigo), which contains 4 mg/kg folate. Starting at 8 weeks of age, WT or *Dnmt3L*$^{+/-}$ males were fed either a high-fat diet (HFD; D12492, Research Diets, NJ, USA) with 60% kcal from fat or a matched-control-diet (MCD; D12450J, Research Diets) with 10% kcal from fat; both diets contained 2 mg/kg folate. MCD is matched with HFD for protein (20% kcal), mineral, vitamin and every other ingredient except for fat and carbohydrate ratios (Supplementary Table 1). The HFD has been previously used and shown to induce weight gain and obesity in mice [50, 51]. Males were fed the diets for 11–13 weeks before breeding, ART or sperm collection.

Spermatogonia, sperm isolation and DNA extraction

Postnatal spermatogonia were isolated using from GOF/deltaPE-Oct4/GFP mice by fluorescence-activated cell sorting as described in Niles *et al.* [52]. Briefly, WT and *Dnmt3L*$^{+/-}$ GFP+ males and females were mated in order to generate GFP+ *Dnmt3L*$^{+/-}$ male offspring. At postnatal day 4, paired testes were removed, decapsulated, digested in a solution of Collagenase I and IV (both at 1 μg/testis; Sigma, ON, Canada) for 10 min at 37°C, dispersed and digested for an additional 10 min. The suspension was centrifuged

at 1800 rpm for 5 min at 4°C, followed by further digestion in 0.25% trypsin–EDTA (Thermofisher, ON, Canada) for 10 min, dispersal, digested for an additional 10 min and centrifuged. This final cell suspension was washed twice and resuspended in sterile phosphate-buffered saline (Thermofisher) with 5 ug/ul DNAse. Flow cytometric analyses and FACS was performed using FACScan and FACSAira, respectively, at the FACS core facility at McGill University and kept frozen at −80°C. DNA was isolated using the QIAamp DNA micro Kit (Qiagen, ON, Canada).

Mature sperm from one of the cauda-epididymides were collected with the swim-out method [47] and kept at −80°C until DNA isolation was performed. Sperm were left at 37°C overnight in a buffer containing 10 mM EDTA, 150 mM Tris, 0.1% sarkosyl, 40 mM dithiothreitol and 2 mg/ml proteinase K. The next day, the lysate was used for DNA isolation using DNeasy Blood & Tissue Kit (Qiagen) according to the manufacturer's protocol.

Reduced representation bisulfite sequencing (RRBS)

Sperm DNA libraries for RRBS (n = 6 per group) were prepared according to a previously published protocol using a gel-free technique [53–55] with minor modifications; quantitative PCR (qPCR) was used instead of regular PCR during cycle optimization to decrease the number of amplification cycles [56]. We used 500 ng sperm DNA as a starting material and performed overnight MspI digestion (New England Biolabs-NEB, MA, USA). Digested samples were end-repaired and A-tailed using Klenow fragment (NEB), followed by a clean-up using Agencourt AMPure XP magnetic beads (Beckman Coulter, CA, USA). Methylated Adaptors (NEB) were ligated to cleaned DNA and bisulfite conversion was performed twice using EpiTect Bisulfite kit per manufacturer's protocol (QIAGEN). Bisulfite converted DNA was used in qPCR by the addition of 1 μl of SYBR Green Nucleic Acid Stain 5X (Thermofisher) to the qPCR mix KAPA HiFi HotStart Uracil+ Kit (KapaBiosystems, MA, USA). Optimal cycle numbers were determined for each sample using LightCycler 96 System (Roche, ON, Canada). Large scale qPCR using previously determined optimal cycle number for each sample and additional bead clean up was performed before sequencing.

Prepared RRBS libraries were sent to Centre d'expertise et de services (CES) Génome Québec (QC, Canada). Twelve samples were multiplexed and were sequenced in one lane with paired-end sequencing using NovaSeq 6000 PE150 bp (Illumina, CA, USA). Raw data processing was performed as previously described [23] using bsmap (version 2.6) [57]. MethylKit software (version 1.8.1) was used for differential methylation analysis using the Benjamini-Hochberg false discovery rate (FDR)-based method for *P*-value correction (q = 0.01) [58]. CpGs with 10X coverage in all samples and a difference of at least 10% between compared groups were identified. Alterations in DNA methylation were assessed as follows: methylKit produces lists of 1) differentially methylated cytosines (DMCs) and 2) differentially methylated 100 bp tiles (DMTs) containing at least two CpGs; to examine for larger regions of differential methylation 3) DMCs that were found to be within 100 bp apart were merged to obtain merged differentially methylated regions (DMRs). Any DMCs that were not merged, remained as single DMCs. This was accomplished using the emergeBed -d function of bedtools (version 2.29.2). All annotations were performed with HOMER software (version 4.9.1) [59]. Common DMTs were determined using the intersectBed -u function of bedtools (version 2.29.2). Gene ontology enrichment analysis using merged DMRs compared against merged background regions (all tested sites/tiles merged that are within 100 bp apart) was performed using a web based functional enrichment analysis tool, WebGestalt (WEB-based GEne SeT AnaLysis Toolkit) [60]. The proportion of overlaps between merged hypomethylated DMRs and repeats was identified using the RepeatMasker program (version 4.1.1, http://www.repeatmasker.org) [61].

Glucose and insulin tolerance tests

Metabolic tests were performed between 8–10 weeks of starting the diets, one week apart. Glucose tolerance test (GTT) was performed following an overnight (~16 h) fasting with free access to water. Time 0 glucose levels were measured by nicking the tail and measuring the blood with a glucometer (Accu-Check Aviva Nano). 2 mg/kg filter-sterilized 20% glucose solution (D-glucose, G7021, Sigma) was administered intraperitoneally (IP) and blood glucose levels were measured and recorded again at 15, 30, 60 and 120 min.

Insulin tolerance test (ITT) was performed following a ~6 h fasting with free access to the water. After blood glucose was measured for time point 0, an IP injection of 1 IU/kg insulin (Insulin solution human 10 mg/ml, I9278, Sigma) was done. Blood glucose levels were measured at 15, 30, 60 and 120 min with a glucometer (Accu-Check Aviva Nano).

Red blood cell folate

Whole blood was collected in EDTA tubes by cardiac puncture at necropsy. Blood was centrifuged at 1445 g for 5 min and the plasma collected. Red blood cell pellets were frozen and shipped on dry ice to Health Canada for analysis. The *Lactobacillus casei* microbiological assay was used to measure red blood cell (RBC) folate as previously described [62]. RBC folate content was normalized to total protein, which was determined using the modified Lowry assay [63].

ART and natural mating

ART was performed according to previously published protocols and the Jackson Laboratory method [12, 64, 65]. Eight week old CF1 females were superovulated by IP injection of 5 IU of pregnant mares' serum gonadotropin (PMSG, 367222, Milipore, ON, Canada) followed by 5 IU human chorionic gonadotropin (hCG, 230734, Milipore) [9]. IVF was performed in human tubal fluid (HTF, MR-070-D, Millipore) using sperm from WT or *Dnmt3L*$^{+/-}$ C57BL/6 males on diets (MCD or HFD) and superovulated CF1 female oocytes. Fertilized oocytes were transferred to a potassium simplex optimization medium with 1/2 amino acids (KSOM, MR-106-D, Millipore) under mineral oil and cultured at 37°C, humidified and reduced oxygen conditions (5%O_2, 5%CO_2 and 90%N_2) for 4 days. Blastocysts acquired from the embryo culture were transferred to 2.5 days post-coitum (dpc) pseudopregnant recipient CF1 female mice. Ten blastocysts were transferred to each female using a non-surgical embryo transfer (NSET) device (ParaTechs, KY, USA). Embryo transfer day is determined as embryonic day 3.5 (E3.5) and midgestation embryos and placentas were collected 8 days later (Fig. 3A). Fertilization rates were calculated as number of fertilized eggs/number of all eggs and *in vitro* development (IVD) rates were calculated as number of morula or blastocysts/number of fertilized eggs.

For natural mating (NAT), 2 CF1 females were placed into cages with one WT or *Dnmt3L*$^{+/-}$ C57BL/6 male and the day on which we observed a vaginal plug was denoted as E0.5. Midgestation embryos and placentas were collected 10 days later.

Assessment of midgestation embryos and placentas

ART or NAT conceived embryos and placentas were collected at midgestation (E11.5). CF1 female uteri (and corpus hemorrhagicum in the ovaries of NAT females) were analyzed for the number of ovulated oocytes, implantation sites, resorptions, and live embryos to determine pre-and post-implantation losses. Morphological assessment of embryos to determine developmental delays and growth abnormalities was performed as previously described [66], by blinded personnel without knowledge of the source of the embryo to eliminate any bias. Embryos delayed by 2 days or more (i.e. staged E9.5 or less) were denoted as developmentally delayed [11]. Crown-rump length (CRL) and placenta area were measured and recorded during the collection. Collected tissues were snap-frozen on dry ice and stored at −80°C until further use. The sex of the embryos was determined by PCR [66] using the yolk sac and re-confirmed using placenta DNA that was extracted for methylation analysis (see below).

Tissue DNA isolation and pyrosequencing

Frozen placentas were homogenized using mortar and pestle on dry ice and homogenized tissue powder was used for DNA isolation using the DNeasy Blood and Tissue kit (Qiagen) following the manufacturer's protocol. Placenta DNA from female and male embryos, coming from the same litter or same father and embryonic stage-matched between groups (NAT WT n = 20, NAT *Dnmt3L*$^{+/-}$ n = 21, ART WT n = 41, ART *Dnmt3L*$^{+/-}$ n = 40) were used for bisulfite conversion using the EpiTect Bisulfite kit (QIAGEN) per the manufacturer's protocol. Bisulfite converted DNA was used for DNA methylation analysis at four imprinting control regions (*H19*, *Snrpn*, *Kcnq1ot1* and *Peg1*) with bisulfite pyrosequencing as previously described [66].

Statistical analysis

Statistical analysis and graph generation were performed using Graphpad Prism 6.0 (GraphPad Software Inc., CA, USA). The statistical significance threshold was set to $P < 0.05$ for all tests. Categorical variables were tested with Chi-Square Test with Yates' correction. Continuous variables were tested using one-way ANOVA or two-way ANOVA (depending on the number of independent variables) with multiple comparisons.

GTT and ITT results were compared with multiple t-test with Holm-Sidak correction comparing diet groups within the same genotype (Fig. 2C and D).

The differences between CRL and placenta area were calculated by graphing a common slope for both groups and calculating a distance for each point. Distances were then used for Student's t-test to determine if they were statistically different (Supplementary Fig. 7A–C).

Results

Dnmt3L haploinsufficiency but not high fat diet resulted in widespread alterations in DNA methylation patterns in mouse sperm

Eight-week-old C57BL/6 male mice with a *Dnmt3L*$^{+/+}$ (WT) or *Dnmt3L*$^{+/-}$ genotype were fed either a HFD (60% kcal from fat) or a matched control diet (MCD, 10% kcal from fat: fat replaced with cornstarch and matched for all other ingredients, Supplementary Table 1), for 12 weeks. As one cycle of spermatogenesis is ~35 days, the mice were on the diets for two full cycles of spermatogenesis before any analyses were performed. This diet exposure and length has previously been used to induce significant gains in weight as well as obesity and has been demonstrated to induce alterations in sperm histone marks [50, 51]. Sperm were collected from four groups of males, MCD WT, MCD *Dnmt3L*$^{+/-}$, HFD WT and HFD *Dnmt3L*$^{+/-}$ (n = 6/per group) to assess the effects of genotype (*Dnmt3L*$^{+/-}$), diet (HFD), or a combination of the two paternal factors (Fig. 1A, left). Genome-wide DNA methylation analysis was performed using reduced representation bisulfite sequencing (RRBS) (Supplementary Table 2).

First, methylation differences in sperm were assessed by identifying differentially methylated tiles (DMTs), 100 bp stepwise windows that contain at least 2 CpGs. We compared the four male groups (Fig. 1B, Supplementary Table 3 and Supplementary Files 1–3). RRBS revealed 14 974 DMTs for the MCD *Dnmt3L*$^{+/-}$ compared to the MCD WT sperm (genotype effect), with the majority of the tiles showing a loss of methylation (hypomethylation; 14 811, 98.9%) (Fig. 1B, left panel, Supplementary Table 3 and Supplementary File 1). HFD alone had little impact on sperm DNA methylation (diet effect); 523 DMTs were identified when comparing the sperm of WT mice on the HFD vs the MCD (Fig. 1B, left panel, Supplementary Table 3 and Supplementary File 2). The genotype effect on mice fed the HFD (HFD *Dnmt3L*$^{+/-}$ versus HFD WT comparison) induced 17 378 DMTs, almost all showing a loss of methylation (hypomethylation; 17 303, 99.6%—Fig. 1B, left panel. Supplementary Table 3 and Supplementary File 1). Overall, *Dnmt3L*$^{+/-}$ had the most dramatic effect on sperm DNA methylation patterns whereas HFD alone had minimal effects.

Further analysis of the genomic distribution of DMTs indicated that *Dnmt3L*$^{+/-}$ genotype, whether in mice fed MCD or HFD, gave similar results: most of the sperm DMTs were located in intergenic regions (77.6%) followed by intronic (15.7%) and exonic regions (3.6%) (Fig. 1B, upper right). HFD diet-specific DMTs were also mostly found in intergenic regions (60%), though their proportion was lower than those caused by genotype effect; this was followed by a higher proportion of both intronic (24.5%) and exonic regions (9.6%) (Fig. 1B, upper right). Similarly, the magnitude of changes in DNA methylation was comparable in *Dnmt3L*$^{+/-}$ on a MCD or HFD, with ~10% of DMTs exhibiting 20–40% change in methylation (Fig. 1B, lower right). The majority of these larger changes were occurring in areas of intermediate levels of methylation (20–80%) in the WT samples (Supplementary Fig. 1A and B). The minimal effect of the HFD on sperm DNA methylation resulted in methylation changes in the 10–15% range, which were also found to occur in regions of intermediate methylation (Fig. 1B, lower right and Supplementary Fig. 1C).

Next, the effects of *Dnmt3L*$^{+/-}$ on sperm DNA methylation were validated in a separate cohort of mice. Spermatogonia were included to determine whether DNA methylation was affected in *Dnmt3L*$^{+/-}$ mice, closer to the developmental time when DNA methylation is acquired in male germ cells (i.e. in the prenatal prospermatogonia from embryonic days 15.5–18.5). We used *Oct4*-GFP crossed *Dnmt3L*$^{+/-}$ or WT male mice to isolate spermatogonia at postnatal day 4 (Fig. 1A, right side). RRBS revealed many DMTs in *Dnmt3L*$^{+/-}$ compared to WT both in spermatogonia and sperm of this validation cohort (V). Again, we found that the majority of tiles were hypomethylated (Fig. 1C, left) and enriched in intergenic regions (Supplementary Fig. 2A). There were more DMTs in sperm than spermatogonia, consistent with ongoing *de novo* DNA methylation during spermatogenesis. In sperm, ~15% of DMTs exhibited 20–40% changes in DNA methylation, similar to our earlier results (Fig. 1C, right). However, in spermatogonia the proportion of DMTs exhibiting 20–40% changes was found to be greater at ~30%. Similar to the genotype effect found above,

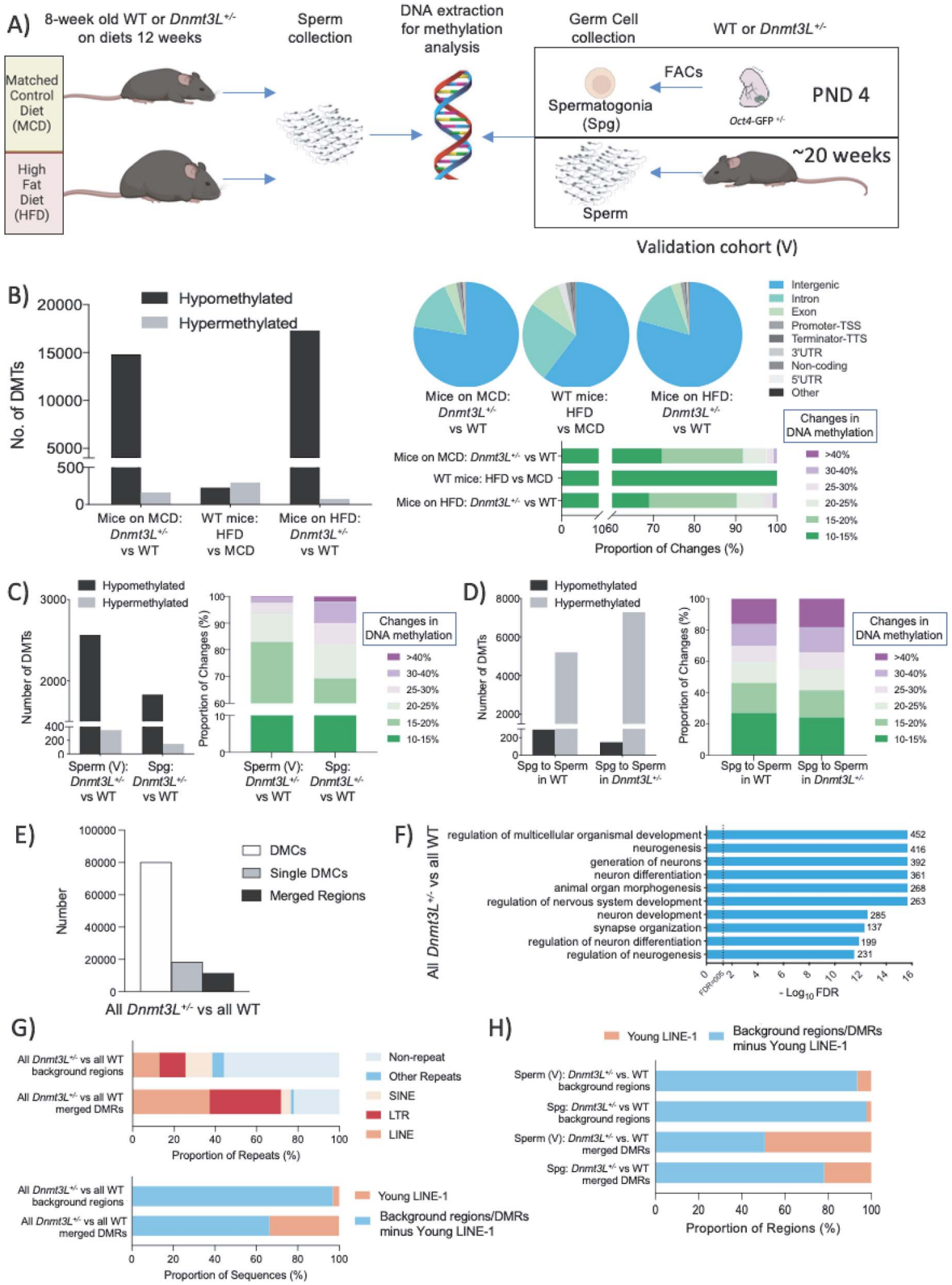

Figure 1. Genome-wide DNA methylation analysis of sperm and spermatogonia. (A) Experimental design of germ cell DNA methylation analysis. WT and *Dnmt3L*$^{+/-}$ mice were fed a MCD or HFD for 12 weeks, following which sperm was collected and DNA extracted for analysis. A sperm validation cohort (V) was also collected, along with postnatal day 4 (PND 4) spermatogonia via fluorescence-activated cell sorting (FACs). (B) Number of 100 bp tiles that are differentially methylated (DMTs) in sperm, between groups comparing the male factors (*Dnmt3L*$^{+/-}$, HFD and the effect of *Dnmt3L*$^{+/-}$ on mice fed HFD; left). Loss of methylation denoted as hypomethylated, whereas gain of methylation denoted as hypermethylated. Genomic distribution of DMTs overlapping with different elements in the genome (top, right). The magnitude of DNA methylation changes (gain and loss) observed at DMTs (bottom, right). Number of DMTs and the magnitude of changes in DNA methylation found (C) in a sperm validation cohort (V) and in spermatogonia (Spg) and (D) in a developmental context from Spg to Sperm from *Dnmt3L*$^{+/-}$ vs WT animals. (E) DMCs that were found within 100 bp were merged to acquire merged DMRs in all *Dnmt3L* haploinsufficient sperm compared to WT (MCD and HFD combined). The number of DMCs, single DMCs and merged regions is shown as a bar graph. (F) Gene Ontology (GO) analysis of merged DMRs identified in all *Dnmt3L* haploinsufficient sperm compared to WT (MCD and

the majority of these larger changes are occurring in areas of intermediate levels of methylation (Supplementary Fig. 1D and E).

Greater increases in DNA methylation were observed during the transition from spermatogonia to sperm in *Dnmt3L*$^{+/-}$ animals

Taking advantage of the isolated spermatogonia data along with that for sperm in the V cohort, we next examined changes in DNA methylation in a developmental context. In WT mice, increases in DNA methylation were found to occur as male germ cells develop (Fig. 1D, left). Interestingly, increases in DNA methylation were more marked in the transition from spermatogonia to sperm in *Dnmt3L*$^{+/-}$ animals compared to the WT group. Altered DNA methylation was found to occur in intergenic (46–51%), intronic (25–24%) and exonic (21–18%) regions from WT and *Dnmt3L*$^{+/-}$ mice, respectively (Supplementary Fig. 2B). During development, larger magnitude changes in DNA methylation occurred, with over 50% of the DMTs showing >20% change in values (Fig. 1D, right). This dramatic increase can be observed in areas of low levels of methylation in spermatogonia, gaining methylation close to 100% in mature sperm (Supplementary Fig. 1F–G).

Tiles that gained methylation during development from spermatogonia to sperm (hypermethylated) in WT and *Dnmt3L*$^{+/-}$ groups were compared. We identified 3564 common tiles: 1585 DMTs gained more methylation in WT compared to *Dnmt3L*$^{+/-}$ while 1979 DMTs gained more methylation in *Dnmt3L*$^{+/-}$ compared to WT, (Supplementary Fig. 2C and D). The genomic distribution of the DMTs was similar to both groups (Supplementary Fig. 2E). Interestingly, the proportion of changes was significantly different over all ranges of DNA methylation in *Dnmt3L*$^{+/-}$ as compared to that of WT (Supplementary Fig. 2F). These results demonstrate that *Dnmt3L* haploinsufficiency leads to loss of DNA methylation in spermatogonia. The increased hypermethylation found when spermatogonia transition to sperm suggest that catch-up methylation was occurring during spermatogenesis in *Dnmt3L*$^{+/-}$ males, consistent with our previous results [52]. However, not all sperm DNA methylation can be recovered during spermatogenesis leading to mature spermatozoa with sperm epimutations.

Dnmt3L$^{+/-}$ -specific merged differentially methylated regions (DMRs) in sperm were associated with neurodevelopment and enriched in young retrotransposons

Since the obesogenic high-fat-diet induced few alterations in DNA methylation compared to *Dnmt3L* haploinsufficiency, we further investigated DNA hypomethylation in the sperm of all WT compared to all *Dnmt3L*$^{+/-}$ males, combining the samples from the MCD and HFD groups. Rather than examining DMTs, we analyzed the number of individual differentially methylated CpGs (DMCs). The total number of DMCs was high for this comparison (80 052 total), with 79 554 hypomethylated DMCs (Supplementary Table 3 and Supplementary File 1). Next, DMCs found in close proximity (≤100 bp apart) were combined into merged differentially methylation regions (DMRs) to determine whether the changes were in isolated single DMCs or grouped into larger regions. Seventy-seven percent of all DMCs could be combined, forming 11 624 merged regions (Fig. 1E). Most merged DMRs were smaller than 200 bp in size, having a mean size of 97 bp; however some merged regions were as large as 1004 bp (Supplementary Fig. 3A, left). As expected, with the hypomethylating effect of *Dnmt3L*$^{+/-}$, the largest regions were those with losses of DNA methylation and contained the greatest number of merged DMCs (Supplementary S3A, right and Supplementary File 4). Similar to the genomic distribution of the DMTs, merged DMRs where mainly characterized as intergenic and were also the largest regions (Supplementary File 4). Additional group comparisons are shown in Supplementary Fig. 3. For instance, 75 169 hypomethylated DMCs were identified when comparing the HFD-*Dnmt3L*$^{+/-}$ group versus the MCD-WT group, the combined genotype and diet effect (Supplementary Table 3 and Supplementary File 3). Again, the majority DMCs (74%) could be combined into merged DMRs with a mean size of 95 bp (largest 1004 bp), with large hypomethylated regions in intergenic regions and containing the largest number of merged DMCs (Supplementary Fig. 3B and Supplementary File 4). In contrast, examining the diet effect when all animals from the HFD were compared to the MCD (*Dnmt3L*$^{+/-}$ and WT genotypes combined), resulted in 999 total DMCs, with the majority being hypermethylated (Supplementary Table 3 and Supplementary File 2). In this case, 78% of altered sites remained as single DMCs; the mean size of merged DMRs was 67 bp with the largest only 260 bp (Supplementary Fig. 3C, left and middle, respectively). For the diet effect, the largest merged DMRs were those of increased methylation and contained the most DMCs (Supplementary Fig. 3C, right and Supplementary File 4). This regional DMR versus isolated DMC analysis further emphasized the more significant impact of *Dnmt3L* haploinsufficiency on sperm DNA methylation patterns versus that of the HFD.

The aim of obtaining merged DMRs was to explore affected genomic regions with potential links to functional impacts. We used these merged regions to perform a gene ontology (GO) term analysis. GO annotation (top 10 most significant pathways) of the affected regions of *Dnmt3L*$^{+/-}$ when compared to WT (MCD and HFD combined) revealed that most were found in and around genes involved in developmental, especially neurodevelopmental pathways (Fig. 1F). Similarly, merged DMRs affected by the HFD *Dnmt3L*$^{+/-}$ compared to the MCD WT were also enriched in neurodevelopmental and neuron function pathways (Supplementary Fig. 3D). HFD-affected merged DMRs as compared to the MCD (*Dnmt3L*$^{+/-}$ and WT combined) were only significantly enriched for a single pathway, the regulation of action potential (Supplementary Fig. 3E).

We next determined whether all the merged DMRs were enriched in repeat elements in the genome, as compared to background regions (i.e. all tested sites/tiles that were merged if within ≤100 bp). When examining the effect of *Dnmt3L*$^{+/-}$, the background regions were mainly found in non-repeats (55%) and with 13% in each LINEs and LTRs (Fig. 1G, top); however, all merged DMRs affected by *Dnmt3L*$^{+/-}$ were enriched for long interspersed nuclear elements (LINEs, 37%) and long terminal repeats (LTRs,

HFD combined). The number next to each bar represents the number of observed genes in the merged DMR list within the given pathway. False discovery rate (FDR) of 0.05 is indicated with a dotted line. (G) Proportion of overlaps between repeat regions in background regions and *Dnmt3L*$^{+/-}$ specific merged DMRs identified using the RepeatMasker program (top). The percentage of evolutionarily young LINE1s (L1Md family of retrotransposons) in the genome or background regions/DMRs minus young LINE-1 elements that are overlapping background regions and *Dnmt3L*$^{+/-}$ specific merged DMRs (bottom). (H) Merged DMRs affected in *Dnmt3L* haploinsufficient vs. WT in a validation cohort (V) of sperm and Spg were overlapped with evolutionarily young LINE-1s (L1Md family of retrotransposons) or the background regions/DMRs not in young LINE-1 elements. *Dnmt3L*$^{+/-}$: *Dnmt3L* haploinsufficient; MCD: matched control diet; HFD: High-Fat Diet; Spg: Spermatogonia; SINEs: Short interspersed nuclear elements; LTRs: Long terminal repeats; LINEs: Long interspersed nuclear elements.

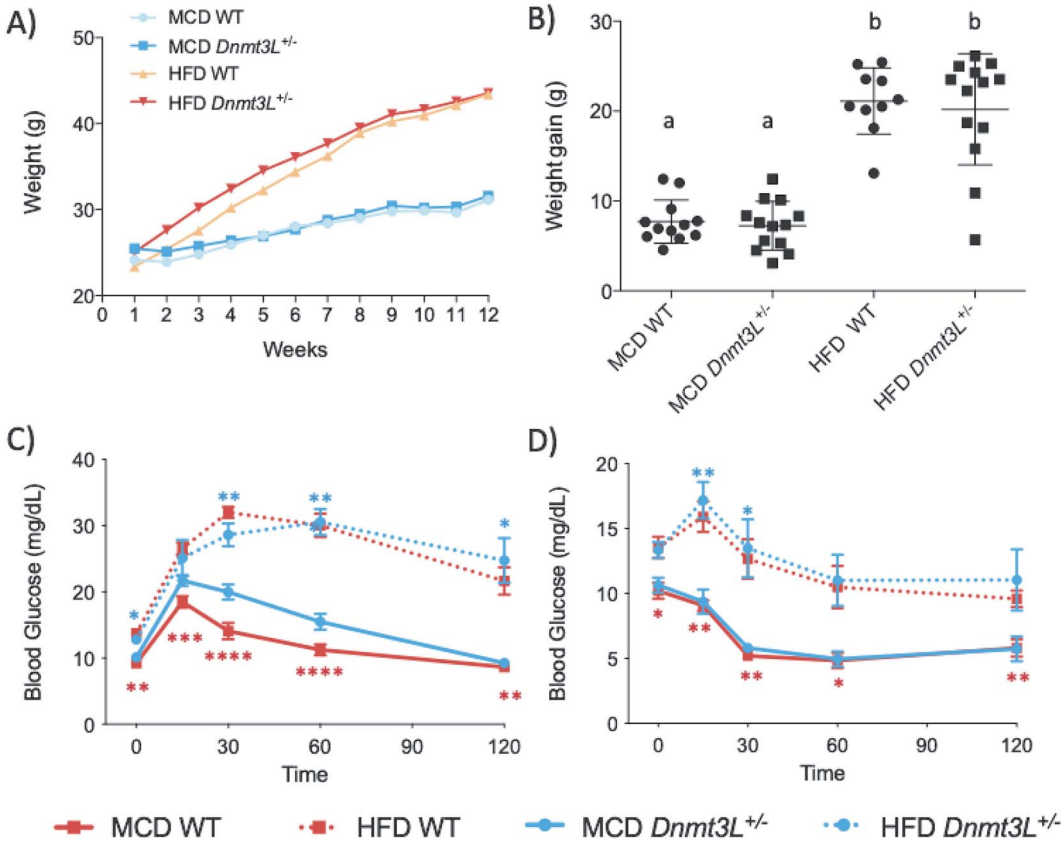

Figure 2. The metabolic effects of high-fat diet (HFD) compared to matched-control diet (MCD). (A) The average weight (g) of male groups at different time points. Animals were weighed weekly for 12 weeks (duration of the diet). (B) Weight gain for each male was plotted to compare different diet and genotype groups. Mean ± SEM are shown, and one-way ANOVA with Tukey's correction for multiple comparisons was used to compare different groups. Groups indicated with the same letter do not show a significant difference whereas groups indicated with a different letter are significantly different. Statistical significance set to $P < 0.05$. (C) Effects of HFD on glucose tolerance in male mice. Change in blood glucose levels after an intraperitoneal (IP) injection of glucose was followed for 120 min with 30 min intervals, (MCD WT n = 7, MCD *Dnmt3L*$^{+/-}$ n = 9, HFD WT n = 7, HFD *Dnmt3L*$^{+/-}$ n = 6, mean ± SEM were plotted). Multiple t-test with Holm-Sidak correction was used to compare glucose levels at different time points between males on a different diet but with the same genotype. (D) Effects of HFD on insulin tolerance in male mice. Change in blood glucose levels after an intraperitoneal (IP) injection of insulin was followed for 120 min with 30 min intervals, (MCD WT n = 7, MCD *Dnmt3L*$^{+/-}$ n = 8, HFD WT n = 7, HFD *Dnmt3L*$^{+/-}$ n = 6, mean ± SEM were plotted). Multiple t-test with Holm-Sidak correction was used to compare glucose levels at different time points between males on different diets but with the same genotype. Statistical significance set to $P < 0.05$. *, $P < 0.05$; **, $P < 0.01$; ***, $P < 0.001$ ****, $P < 0.0001$.

35%). This can also be seen in the combination *Dnmt3L*$^{+/-}$ and HFD effects (Supplementary Fig. 3F). The HFD-specific DMRs were only enriched in LTRs (32% of all merged DMRs vs 13% in background regions) (Supplementary Fig. 3F). Most transposable elements are not capable of transposition in the genome with only some young families having the potential to cause unwanted effects [67, 68]. A relatively younger group of LINE-1 elements, L1Md [23], was analyzed to test for overlaps with all background regions and identified merged DMRs. Interestingly, nearly 38% of all *Dnmt3L*$^{+/-}$ specific merged DMRs overlapped with these young LINE-1 elements compared to about 5% for the background regions (Fig. 1G, bottom). Results were similar for combined *Dnmt3L*$^{+/-}$ and HFD effect merged DMRs (Supplementary Fig. 3G), while HFD-specific merged DMRs were not different from their background regions in terms of young LINE-1 proportions (Supplementary Fig. 3G). In a developmental context, young LINE-1 elements made up a greater proportion of the *Dnmt3L*$^{+/-}$ affected DMTs in sperm as compared to spermatogonia (Fig. 1H). This may suggest that methylation of these types of sequences may not be corrected during spermatogenesis as much as other types of non-repetitive intergenic sequences, which we previously reported as being corrected between the spermatogonial and spermatozoal phases [52]. Our findings here show enrichment of hypomethylated young retrotransposons in the sperm of *Dnmt3L*$^{+/-}$ males, representing a potential contributor to adverse functional consequences for the next generation.

High-fat-diet fed males showed metabolic disturbances but had normal folate levels

In keeping with the literature, HFD groups, independent of their genotype, gained significantly more weight than their MCD-fed counterparts (Fig. 2A and B). Following the 12-week diet period the MCD mice (WT and *Dnmt3L*$^{+/-}$ combined) weighed 31.4 ± 0.5 g, while the HFD mice weighed 43.5 ± 0.8 g; the groups gained approximately 7.5 ± 0.5 g and 20.2 ± 1.1 g, respectively. Testes weights were similar in the HFD and MCD groups, although they were proportionally smaller in the HFD group in relation to body weight (Supplementary Fig. 4A).

Next, we carried out glucose tolerance (GTT) and insulin tolerance (ITT) tests to confirm that our HFD impacted glucose metabolism and insulin concentrations. HFD-fed groups showed significantly higher concentrations of fasting glucose compared to MCD groups (time 0, Fig. 2C). The HFD group also had significantly higher blood glucose concentrations than the MCD group at most time points between 15 and 120 min (Fig. 2C). Following the ITT, MCD-fed animals responded quickly to the insulin

challenge and had lower than baseline glucose concentrations as early as 15 min. Other time points demonstrated a further concentration decrease at 30 min, reaching a plateau (Fig. 2D). In contrast, HFD males exhibited an initial increase in blood glucose and responded more slowly to insulin, 30–60 min post-injection (Fig. 2D).

Folate metabolism via the one-carbon metabolic pathway produces S-adenosyl methionine (SAM), the universal methyl donor for biological methylation reactions such as DNA methylation. Folate requirements may be higher in obese individuals given that circulating folate is often lower than in normal weight individuals [69]. To test whether folate concentrations were affected by the HFD diets, we measured folate in red blood cells (RBC), a marker of chronic exposure. Folate concentrations were not lower in mice in the HFD groups (Supplementary Fig. 4B). Thus, changes in sperm DNA methylation observed in the HFD *Dnmt3L*$^{+/-}$ group cannot be explained by differences in folate concentrations.

ART affected overall pregnancy outcomes and caused developmental delays in midgestation embryos

Sperm from the four groups of males (WT and *Dnmt3L*$^{+/-}$, each with MCD and HFD) were used for *in vitro* fertilization (IVF) (Fig. 3A). In addition to IVF, the ART procedures included superovulation of females, embryo culture to the blastocyst stage and non-surgical embryo transfer to pseudopregnant females. To better elucidate the effect of ART we compared the outcomes to a natural mating group using MCD WT and *Dnmt3L*$^{+/-}$ males. At midgestation (E11.5), embryos and placentas were collected, and embryonic assessments were performed in a blinded fashion.

The number of males used in each group, as well as the ART and pregnancy outcomes, are listed in Fig. 3B. While greater numbers of embryos were collected in the *Dnmt3L*$^{+/-}$ groups, the average numbers of embryos per litter in all groups were not significantly different (range 3.2–3.5). Fertilization rates were high (≥94%) and *in vitro* development (IVD) rates to morula and blastocyst stages ranged from 61–68%; there were no significant differences among the four ART groups (Fig. 3B and Supplementary Fig. 5A and B). The preimplantation loss was significantly higher for all ART groups compared to natural mating (NAT), however, there were no significant differences among ART groups (Fig. 3C). Post-implantation losses were significantly higher (Fig. 3D) and the number of viable embryos lower (Fig. 3E) for the ART groups.

Next, embryonic development was examined. Developmental delay was defined as a delay in the growth of midgestation embryos of ≥2 days. Amongst the over one hundred embryos in each NAT group, there were no delayed embryos in the WT group and only one in the *Dnmt3L*$^{+/-}$ group (Fig. 3F and Supplementary Fig. 6A). In contrast, all ART groups compared to NAT groups showed significantly higher numbers of delayed embryos including those coming from different litters and different fathers (Fig. 3F and Supplementary Fig. 6B). Numbers of delayed embryos were similar among all the ART groups, even when we combined diets (MCD + HFD) and compared WT and *Dnmt3L*$^{+/-}$ (Fig. 3F, rightmost bars). Together, the results indicate that ART caused a significant increase in developmentally delayed embryos at midgestation independent of paternal factors.

Both human and mouse studies have shown that ART can impact fetal size, often resulting in smaller offspring when compared to naturally conceived offspring [70, 71]. We measured crown-rump length (CRL) as well as placenta areas of collected staged midgestation embryos to see if the paternal factors, in conjunction with ART, further exacerbated effects on embryo and placenta sizes. While there were decreases in CRL of ART conceived embryos compared to NAT embryos, the placenta areas were similar between the two groups (Supplementary Fig. 7A). Similarly, the ART and *Dnmt3L*$^{+/-}$ combination induced the same effects: a decrease in embryo CRL but not in placenta size (Supplementary Fig. 7B). The combination of all factors, ART, HFD and *Dnmt3L*$^{+/-}$ not only led to a decrease in embryo size, but also resulted in an impact on placenta size, such that placentas were larger early in development (E9.5-E11.25) and smaller later in development compared to NAT WT mice on MCD (E11.25-E12.0), (Supplementary Fig. 7C). The latter results provide evidence suggesting that ART in combination with both paternal factors impact growth parameters in the fetoplacental unit at midgestation.

Higher incidence of morphological abnormalities in ART embryos from *Dnmt3L*$^{+/-}$ fathers

Midgestation embryos were evaluated for morphological abnormalities. Abnormalities including neural tube defects, craniofacial malformations, laterality defects, and anterior–posterior developmental discordance were observed in all groups (Fig. 4A). NAT groups (both WT and *Dnmt3L*$^{+/-}$) showed the lowest number of abnormalities (Fig. 4B and C), as did the ART WT groups (both HFD and MCD; Fig. 4B and D, left panels). Notably, ART groups with *Dnmt3L*$^{+/-}$ fathers had a significantly greater proportion of abnormal embryos (14.9–20.4%) compared to WT fathers (5.7–8.4%), for MCD and HFD, respectively (Fig. 4D and E). The morphologically abnormal embryos observed were spread over several litters coming from different fathers (Fig. 4C and D). An examination of the different types of abnormalities amongst the groups showed that craniofacial abnormalities were significantly higher in the ART HFD *Dnmt3L*$^{+/-}$ group and laterality defects were significantly higher in the ART MCD *Dnmt3L*$^{+/-}$ group (Fig. 4E). Taken together, the incidence of embryonic abnormalities amongst NAT *Dnmt3L*$^{+/-}$ male sired litters was no different from those from the NAT WT males; it was only when ART was used for conception that the incidence of embryonic abnormalities exhibited a 3-fold increase *Dnmt3L*$^{+/-}$ fathers. The results indicate a cumulative adverse effect of paternal *Dnmt3L*$^{+/-}$ and ART.

ART and paternal *Dnmt3L*-haploinsufficiency impacted imprinted gene control region (ICR) methylation in the placenta

Proper methylation of imprinted genes is crucial for embryonic and placental development and growth. We and others have shown that the imprinting control regions (ICRs) of imprinted genes are particularly susceptible to perturbation after ART, with the placenta being more vulnerable than the embryo to such imprinted gene perturbations [12–14, 66, 72]. Here, with placentas from normal embryos, we first investigated both the effect of the conception method (NAT and ART) as well as the paternal factor *Dnmt3L*$^{+/-}$ in mice fed MCD. The placenta ICR methylation of *Snrpn, Kcnq1ot1, Peg1* (maternally methylated imprinted genes) and *H19* (a paternally methylated imprinted gene) was examined using bisulfite pyrosequencing. For all imprinted genes, ICR methylation levels were lower, and variances were higher in the ART group compared to the NAT group (Fig. 5A and B). We did not identify a significant genotype effect on imprinted gene methylation levels either alone or in combination with the conception method (Fig. 5A). In contrast, for DNA methylation variances, there was a significant interaction between paternal *Dnmt3L*$^{+/-}$ genotype and conception method for *H19*, *Peg1* and

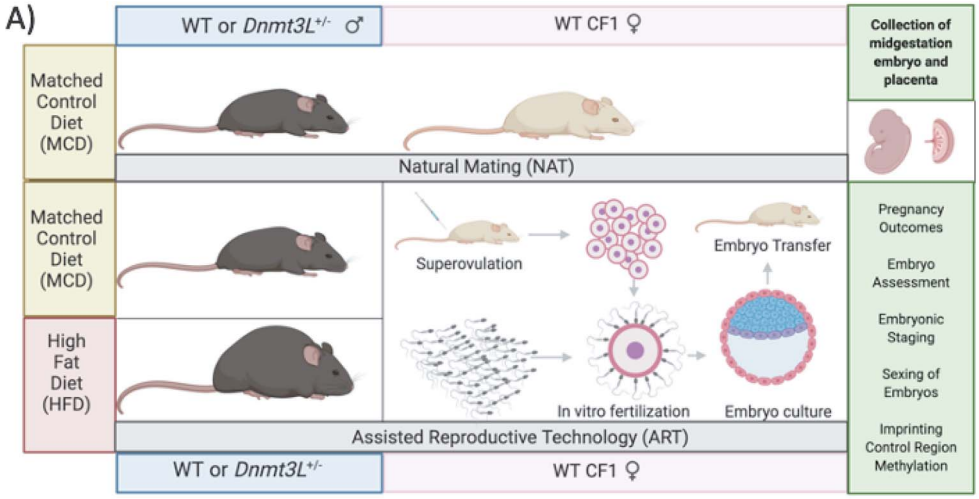

B)

Group	Males	Mean fertilization rate (%)	Mean *in vitro* dev. rate (%)	Number of litters	Number of live mid-gestation embryos (%)
NAT MCD WT	11	-	-	11	154 (90)
NAT MCD *Dnmt3L*$^{+/-}$	10	-	-	10	142 (94)
ART MCD WT	12	94.9 ± 1.7	60.7 ± 6.1	34	107 (31)
ART MCD *Dnmt3L*$^{+/-}$	13	94.0 ± 1.8	65.4 ± 5.0	38	134 (35)
ART HFD WT	10	94.1 ± 1.2	67.8 ± 5.1	32	102 (32)
ART HFD *Dnmt3L*$^{+/-}$	12	94.2 ± 1.8	63.9 ± 4.9	42	145 (35)

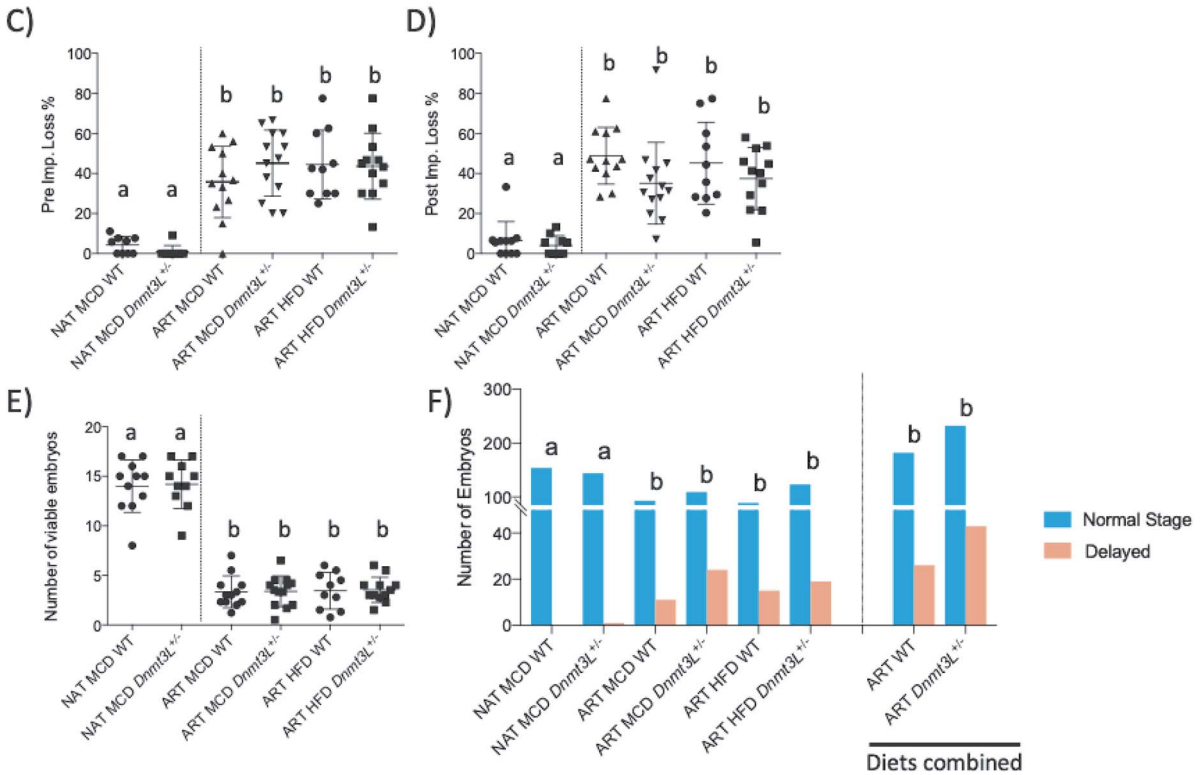

Figure 3. Analysis of outcomes in midgestation embryos produced through either natural mating (NAT) or assisted reproductive technologies (ART). (A) Experimental design of embryo production by NAT or ART from males with different factors. Natural mating only performed with males fed the matched control diet (MCD) whereas ART is also performed with males on a high-fat diet (HFD). ART involved superovulation, *in-vitro* fertilization, embryo culture and embryo transfer. (B) The number of males used in each group, fertilization rates (mean ± SEM) and *in vitro* development rates (mean ± SEM) are listed along with the resulting litter and live embryo numbers. Fertilization rate refers to the proportion of oocytes which have been fertilized; *in vitro* development rate refers to the proportion of fertilized embryos which have developed into blastocysts. Percentage of live embryos, in brackets, is calculated using the number of ovulation sites for NAT groups and the number of blastocysts transferred (10 in each female recipient) for ART groups. (C) The percentage of pre-implantation loss is calculated for the NAT groups by subtracting the number of implantation sites from the number of ovulation sites and for the ART groups, by subtracting the number of implantation sites from the number of blastocysts transferred (10 in each female recipient) (D) Post-implantation loss was calculated by subtracting the number of live embryos from the number of implantation

Snrpn (Fig. 5B). Next, we looked at placental ICR methylation levels amongst the ART groups to test for the effects of individual factors *Dnmt3L*$^{+/-}$ and HFD, and their combination (Supplementary Fig. 8A–D). We did not observe any effect of fathers' genotype, diet, or their combination on offspring placenta ICR methylation levels.

We previously showed that female placentas were more susceptible than those of males to the effects of ART on ICR methylation [14]. Therefore, we investigated the ICR methylation levels in female and male matched placenta samples from all groups. For all imprinted genes examined, ICR methylation levels were significantly lower in both male and female placentas from ART compared to NAT (Supplementary Fig. 9A–D). Paternal *Dnmt3L*-haploinsufficiency was associated with DNA hypomethylation at the *Peg1* ICR for female but not male placentas (Supplementary Fig. 9C); a similar trend was seen for *Snrpn* (Supplementary Fig. 9D). No sex-specific effects were seen for *H19* or *Kcnq1ot1* (Supplementary Fig. 9A and B). Thus, while conception method had the most marked impact on imprinted genes in the placenta, there was evidence that paternal *Dnmt3L*$^{+/-}$ genotype could exacerbate some of the ART effects for imprinted genes.

Discussion

Both human and mouse studies indicate there is a small, but significant, increased risk of negative embryonic outcomes associated with the use of ART [2]. While many studies have examined the techniques themselves, the contribution of underlying infertility of the parents has not been extensively studied [4, 16, 17]. Here, we studied two factors linked to male infertility, a HFD to model obesity and *Dnmt3L* haploinsufficiency as a genetic model. In this proof-of-concept mouse study, we determined whether these factors, alone or in combination, 1) affected the sperm epigenome and 2) had a synergistic effect on embryonic outcomes in the next generation, when ART was used as the method of conception. We demonstrated that *Dnmt3L* haploinsufficiency, but not HFD, resulted in sperm epimutations, specifically marked DNA hypomethylation, particularly for young retrotransposons. Neither paternal *Dnmt3L* haploinsufficiency (naturally conceived) nor ART (from WT males) alone increased the incidence of malformations in midgestation embryos. However, the combination resulted in a significant increase in the incidence of abnormal embryos. Our study shows that a paternal factor associated with underlying sperm DNA methylation abnormalities combined with ART results in a worsening of offspring outcomes.

The sperm epigenome can be affected by various factors such as diet, environmental toxins, and genetic mutations, resulting in abnormal outcomes in offspring [18–23]. Obesity is an epidemic, with the prevalence having approximately doubled since the 1980s [73]. It has been shown to lead to many health problems, including infertility. Indeed, the number of obese men seeking fertility treatment has seen a dramatic increase [42]. Paternal HFD and obesity can affect offspring phenotype causing metabolic, reproductive, and cardiovascular problems [47, 51, 74], indicating underlying abnormalities in the germ cells. While others have reported alterations in sperm DNA methylation as a result of HFDs [40, 41, 75], our results found that HFD alone had a minimal impact on sperm DNA methylation patterns. Other studies have reported effects on other sperm epigenetic modifications such as small non-coding RNAs [48, 76] or histone modifications such as H3K4me3 [51]. Thus, it is possible that in our mouse model, the HFD may have led to more marked effects on epigenetic marks other than DNA methylation, and would require further exploration.

DNMT3L, while lacking catalytic DNA methyltransferase activity, plays a vital role in germ cell development, imprinted gene methylation and fertility. It is expressed in prospermatogonia starting at E12.5, when male germ cell-specific DNA methylation patterns are established [77]. *Dnmt3L* homozygous knockout animals show complete sterility due to meiotic catastrophe [34]. Male mice haploinsufficient for *Dnmt3L* are fertile, however, their germ cells demonstrated abnormal XY chromosome compaction and post-meiotic gene expression abnormalities [78]. The latter findings suggested that there may also be DNA methylation abnormalities in the sperm of *Dnmt3L*$^{+/-}$ mice. Using a DNA methylation analysis technique targeting a small number of loci, we previously showed that *Dnmt3L*$^{+/-}$ male mice have decreased DNA methylation in E16.5 germ cells. However, methylation levels in mature spermatozoa returned to normal in *Dnmt3L*$^{+/-}$ mice when compared to their WT littermates [52]. DNA methylation has not yet been examined at a genome-wide level in sperm of *Dnmt3L*$^{+/-}$ mice. In the current study, the use of a next generation sequencing technique revealed widespread alterations in DNA methylation in *Dnmt3L*$^{+/-}$ postnatal day four spermatogonia and mature sperm. The vast majority of these were decreases in methylation. From these hypomethylated regions, GO analysis demonstrated that terms related to development, especially neurodevelopmental pathways, were enriched. Inheritance of these aberrant epigenetic marks could potentially affect subsequent generations. Indeed, *Dnmt3L* is a paternal effect gene, where wildtype offspring from *Dnmt3L*$^{+/-}$ fathers showed a rare but increased incidence of X chromosome aneuploidy [35]. Future studies should examine whether there are more subtle health effects in the progeny of *Dnmt3L*$^{+/-}$ mice, in particular neurological phenotypes.

Using the *Dnmt3L*$^{+/-}$ animals, we showed that many regions demonstrating hypomethylation were significantly enriched for repetitive elements, in particular, groups of young LINE-1 elements. DNA methylation is one mechanism used in the long-term silencing of retrotransposons. This is important, as evidenced by the fact that such sequences maintain their methylation during the two windows of DNA methylation reprogramming in pre-implantation and germ cell development [24]. In DNMT3L-deficient male germ cells, reactivation of retrotransposons leads to germ cell death. The prospermatogonia of *Dnmt3L*$^{-/-}$ mice show demethylation and re-expression of LINE-1s and the intracisternal A particle (IAP) class of LTR elements [34]. Altered methylation at retrotransposons has also been observed in models of 5,10-methylenetetrahydrofolate reductase (MTHFR) deficiency. This is a crucial enzyme in the one carbon metabolism pathway and is important for methylation reactions. A common genetic variant of *MTHFR* in humans is associated with increased incidences of various disorders, including male infertility [79]. In a mouse model with MTHFR deficiency, our lab has shown that the demethylation of young LINE-1 retrotransposons in sperm persisted through

sites. (E) The number of live embryos in each experimental group. (F) The number of normally developed and developmentally delayed embryos in each experimental group were compared. For data in panels C and D, one-way ANOVA with Kruskal-Wallis for multiple comparisons was used. For data in panel F, Chi-square test was used. Statistical significance was set to $P < 0.05$. Groups indicated with the same letter do not show significant difference whereas groups indicated with a different letter are significantly different.

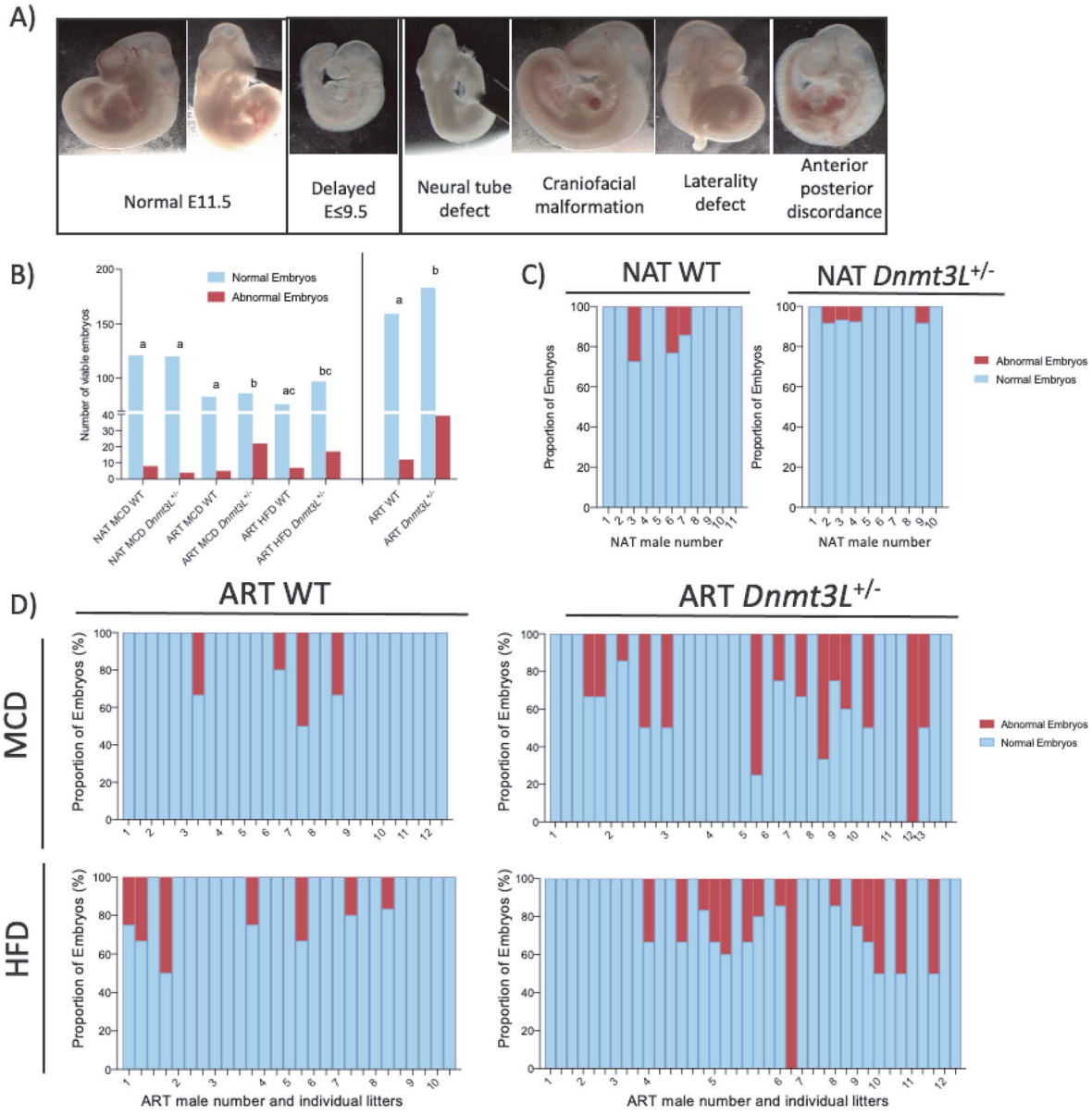

E)

Group	Frequency of abnormalities: Neural Tube	Craniofacial	Laterality	Anterior-posterior discordance	Heart	Other	Total # of Normal Embryos	Total # of Abnormal Embryos (%)
NAT MCD WT	3	1[a]	3[a]	2	0	0	121	8 (6.2)
NAT MCD *Dnmt3L*$^{+/-}$	2	1[a]	1[a]	1	0	0	120	4 (3.2)
ART MCD WT	0	1[a]	2[a]	2	0	0	83	5 (5.7)
ART MCD *Dnmt3L*$^{+/-}$	4	5[ab]	12[b]	4	2	1	86	22 (20.4)
ART HFD WT	2	4[ab]	1[a]	2	1	0	76	7 (8.4)
ART HFD *Dnmt3L*$^{+/-}$	3	9[b]	3[a]	3	1	1	97	17 (14.9)
ART WT (MCD+HFD)	2	5[ab]	3[a]	4	1	0	159	12 (7.0)
ART *Dnmt3L*$^{+/-}$ (MCD+HFD)	7	14[b]	15[b]	7	3	2	183	39 (17.6)

Figure 4. Analysis of morphological abnormalities observed in experimental groups. (A) Examples of lateral and posterior view of normal E11.5 embryo in comparison to developmentally delayed or different morphologically abnormal embryos. (B) The number of morphologically normal (can include developmentally delayed, but normal looking) or abnormal embryos were compared in each experimental group. Fisher's exact test is used to test the significant changes in abnormal embryo numbers compared to normal embryo numbers in different experimental groups. Groups indicated with the same letter do not show significant differences whereas groups indicated with a different letter are significantly different. Statistical significance set to $P < 0.05$. (C) The proportion of abnormal embryos from naturally mated males (numbered from 1 to 10/11) with or without *Dnmt3L* haploinsufficiency is plotted on ratio graphs. (D) The proportion of abnormal embryos from each ART males (numbered from 1 to 10–13) with different male factors (with or without *Dnmt3L* haploinsufficiency, MCD or HFD fed) plotted on ratio graphs; each bar represents an individual litter obtained from each male. (E) Frequency of type of abnormalities observed in different groups. Groups indicated with the same letter do not show significant differences whereas groups indicated with a different letter are significantly different. Statistical significance set to $P < 0.05$, Fisher's exact test.

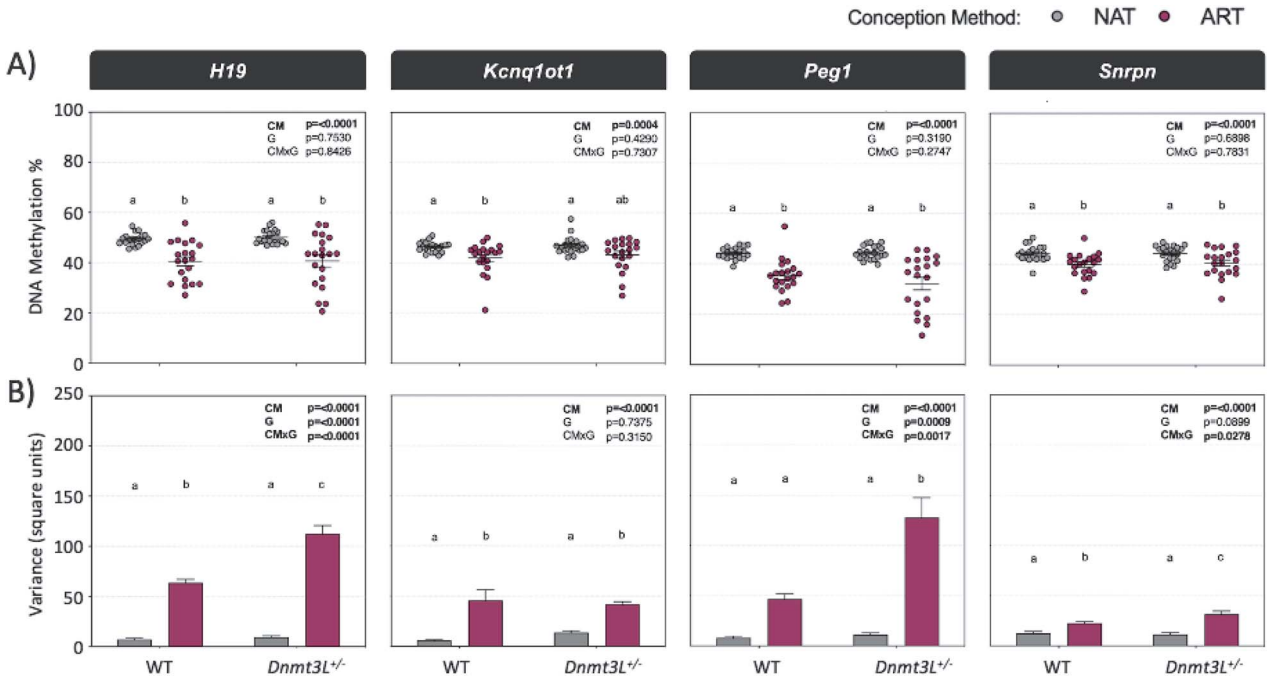

Figure 5. The effect of conception method and paternal genotype interaction on offspring DNA methylation at imprinting control regions (ICRs) in midgestation placenta. (A) Bisulfite pyrosequencing was performed at ICRs of *H19*, *Kcnq1ot1*, *Peg1* and *Snrpn* genes comparing placentas produced by ART or NAT from fathers with WT or *Dnmt3L*$^{+/-}$ genotype. Each dot represents a placenta of a midgestation embryos (NAT WT n = 20, NAT *Dnmt3L*$^{+/-}$ n = 21, ART WT n = 20, ART *Dnmt3L*$^{+/-}$ n = 20). (B) The variance of each group was plotted as a bar graph and two-way ANOVA was performed to determine the effect of conception method, paternal genotype and their interaction; *P* values are shown on the top right for each graph. Tukey's multiple comparison test was also performed to compare the groups to one another; groups indicated with the same letter do not show significant differences, whereas groups indicated with a different letter are significantly different. Statistical significance was set to $P < 0.05$. CM: Conception Method; G: Genotype, CMxG: Conception method and genotype interaction.

epigenetic reprogramming, which takes place during early development. This enzyme deficiency resulted in a worsening of reproductive phenotypes in the next generation [23]. Interestingly, both DNMT3L and MTHFR are expressed during the critical window of male germ cell development, when DNA methylation patterns are being established [77, 80]. Thus, it is possible that in the *Dnmt3L*$^{+/-}$ model, altered DNA methylation at retrotransposons may be inherited by offspring of the next generation.

Several human epidemiologic and molecular studies have suggested that parental infertility can contribute to the adverse outcomes in offspring associated with ART. For instance, a recent study found increased neonatal intensive care unit admissions and large-for-gestational-age (LGA) babies in births following ART in women with diabetes mellitus (DM) compared to the group without DM [81]. Another maternal factor, polycystic ovary syndrome, when combined with ART, resulted in an increased risk for LGA, miscarriage and preterm birth [82]. Fewer studies have examined how paternal factors associated with infertility affect ART outcomes. An early study attributed errors of imprinted gene methylation in sperm to the increased risk of imprinting disorders following ART [17]. A more recent study from our group showed that paternal age and male factor infertility, in combination with IVF/ICSI, were associated with an exacerbation of placental DNA methylation defects in the next generation [83]. This suggested a cumulative effect for ART and underlying infertility. In human studies, teasing out effects of parental infertility and ART techniques on the offspring is challenging. The use of controlled animal models can help us to better understand whether individual defined infertility factors, coupled with ART, can increase risks to the offspring. Indeed, in a mouse study emulating female infertility, we previously demonstrated that a maternal factor, *Dnmt1o* haploinsufficiency in oocytes, resulted in an increased incidence of embryonic abnormalities and epigenetic perturbations following superovulation [66]. There are few animal models studying the combinatory effect of paternal factors and ART [84].

We and others have investigated the effects of ART alone on offspring outcomes in the mouse model. Results presented here, using wildtype mice, confirm our previous study reporting increases in developmental delay following ART compared to natural mating, but no significant increases in the numbers of abnormal embryos at midgestation [14]. In the current study the addition of paternal factors (HFD and *Dnmt3L*$^{+/-}$ genotype) to ART did not exacerbate the effects of ART on developmental delay. However, there were subtle effects of both paternal factors on growth parameters in the fetoplacental unit at midgestation. In addition, an exacerbation of the ART effects was seen for some imprinted genes (i.e. increased variance) in placentas. These more subtle findings suggest it will be important to examine placental function in more detail as well as offspring health postnatally.

While we did not observe a difference in developmental delay with the addition of paternal factors, we found that *Dnmt3L*$^{+/-}$ increased the proportion of abnormal embryos when combined with ART. In particular, craniofacial and laterality abnormalities were found to be significantly increased in embryos fathered by *Dnmt3L*$^{+/-}$ sires using ART. Interestingly, differential methylation in genes related to development and neurodevelopmental pathways was found in sperm from our current mouse model. As offspring outcomes were similar after natural mating of *Dnmt3L*$^{+/-}$ and WT males, the abnormalities observed were unlikely to be due to the genetic disruption alone, but instead to its combination with ART.

HFD did not affect the frequency of ART-dependent developmental abnormalities. HFD and male obesity have been shown to affect adult offspring phenotype causing metabolic, reproductive, and cardiovascular problems [47, 51, 74]. For our model, genome-wide DNA methylation analysis of ART conceived midgestation embryos from HFD fathers might provide insight into their potential to develop health problems later in life. Additionally, future studies could focus on offspring development and health throughout adulthood to further explore this interaction.

The proper monoallelic expression of imprinted genes, controlled by several mechanisms including DNA methylation, is essential for embryonic development and growth. In mice, superovulation alone has been shown to affect imprinted gene methylation. Our previous results, along with others, have shown ICRs in mice to be susceptible when challenged with ART, particularly in the placenta as compared to the embryo [12–14, 66, 72]. In a recent human study a paternal age effect on placental imprinting was reported [85]. We therefore examined DNA methylation at ICRs in placenta from normal midgestation embryos. Consistent with previous studies, all ICRs in the placenta were affected by ART and showed decreased mean methylation. We further explored the effect of paternal factors on ICR methylation, however, other than sex-specific effects on ICR DNA methylation level at one imprinted gene, neither HFD nor *Dnmt3L*$^{+/-}$ or their combination led to a further deterioration of methylation levels. To more fully examine a role for perturbed imprinting in contributing to the birth defects associated with the combination of the paternal *Dnmt3L*$^{+/-}$ genotype and ART, future studies examining both normal and abnormal embryos and placentas would be required.

Hyperstimulation of ovaries using exogenous hormones results in lower quality oocytes that can, upon fertilization, lead to lower implantation rates, increased post-implantation loss, lower fetal weight, and delayed postnatal growth, indicating that superovulation may result in the release of suboptimal quality oocytes [86]. Embryo culture is another ART procedure reported to induce epimutations [13, 72, 87–89]. This procedure coincides with critical time points of epigenetic reprogramming in the embryo, when almost all DNA methylation is erased except at imprinted genes and some retrotransposons. We propose that after natural mating, aberrant epigenetic marks found within sperm from *Dnmt3L*$^{+/-}$ males may be corrected by compensation mechanisms operating in normally ovulated mature oocytes, leading to normal development. In contrast, after ART, due to compromised quality of oocytes and embryos, proper epigenetic programming in pre- and postimplantation development is impaired, such that epimutations in sperm from *Dnmt3L*$^{+/-}$ fathers are not corrected. Hypomethylation leading to aberrant expression of young retrotransposons during early embryogenesis is a potential explanation for the increase in abnormalities in the ART-conceived offspring of *Dnmt3L*$^{+/-}$ fathers. Indeed, one study has demonstrated that ART procedures can alter the expression of transposable elements in preimplantation embryos [90]. Another group has demonstrated that early embryo culture until the morula stage, resulted in decreased methylation of the most abundant transposable element classes: LINEs, SINEs and LTRs [91]. In addition, activation of LINE-1 retrotransposons in early embryonic development (after the 2-cell stage) is associated with developmental arrest and morphological abnormalities in pre-implantation embryos through decondensation of chromatin [92]. Interestingly, an increase of H3K4me3 marks was observed in complete *Dnmt3L* knockout mice at promoter regions of transposable elements in meiotic cells [36]. Therefore, in the *Dnmt3L*$^{+/-}$ model in combination with ART, reactivation and abnormal expression of young retrotransposons may arise through altered DNA methylation or other epigenetic marks (such as H3K4me3). Occurring at developmentally inappropriate stages, especially during the vulnerable embryo culture stage, this may cause genomic instability, abnormal chromatin compaction, gene expression or transcription factor binding, leading to an increased occurrence of embryonic abnormalities at midgestation. Future studies are required to confirm if the demethylated young retrotransposons that we observed in sperm, are indeed activated and expressed in ART blastocysts coming from *Dnmt3L*$^{+/-}$ fathers, and whether other epigenetic mechanisms are also altered.

There are several limitations to our study. As stated previously, we only found minor changes in sperm DNA methylation due to HFD. While the RRBS technique allows for the interrogation of ~1 million CpG sites, this represents only 5% of the ~20 million found in the mouse genome. As well, our diets were given to mice as adults, from 8–20 weeks of age. However, obesity in humans often occurs over decades sometimes beginning in childhood. Therefore, the timing and duration of the diets given in our animal model, as compared to a possible lifetime of obesity seen in the human population, may yield different effects on the sperm epigenome. One other limitation is our timepoint studied. Here, and in our other studies investigating the effect of ART, we examined only the mid-gestation timepoint (E11.5), examining embryo and placental size and weight. We have also previously reported methylation defects caused by ART in both tissues, with the placenta being more severely affected [14, 66]. Others have looked at embryonic and extra-embryonic tissues later in gestation, where an overgrowth of the placental junctional zone was observed following ART procedures [12, 15, 91]. It would therefore, be intriguing to examine whether paternal factors in combination with ART have an effect on placental structure at early and later times in development. Similarly, as mentioned previously, GO analysis results pointed to neurodevelopmental pathways being affected and examination of health effects in the progeny at different timepoints would be of interest as well.

Findings in this study may have clinical relevance for men with underlying gene defects that result in sperm epimutations who also use ART to conceive their children. For instance, *DNMT3L* mutations have been reported in men in association with fertility problems, however the number of patients in these studies is low [17, 27–29]. We currently don't know the prevalence of *DNMT3L* mutations in the male ART population and whether or not they affect sperm DNA methylation patterns. The *MTHFR* 677C>T is a common polymorphism that has been reported to be enriched among infertile men in some populations and is also associated with DNA methylation alterations in sperm [93, 94]. Naturally conceived pregnancies from fathers with the *MTHFR* 677C>T polymorphism have a significantly higher risk of recurrent pregnancy loss and early spontaneous abortion [95, 96]. Similar to DNMT3L when combined with ART, paternal *MTHFR* gene polymorphisms may also lead to an exacerbation of adverse outcomes in embryos. Future animal model and clinical studies are needed to more thoroughly address this question, but ART clinics may need to consider implementing screening technologies to identify these mutations as well as sperm epimutations to improve embryonic outcomes.

Author contributions

J.T., G.K. and D.C. designed the study. G.K., J.M., S.R., M.F. and D.C. performed the main experiments and/or analyses of data. F.M and A.J.M. performed folate analysis. G.K., D.C. and J.T. wrote the

manuscript. All authors revised the manuscript. All authors read and approved the final manuscript.

Acknowledgements

We would like to thank the Centre d'expertise et de services (CES) Génome Québec for the sequencing of RRBS libraries. We would also like to thank Drs Chaowu Xiao and Jayadev Raju of Health Canada for their critical internal review of the manuscript and providing helpful comments and suggestions.

Supplementary data

Supplementary data is available at *HMG Journal* online.

Conflict of interest statement: The authors declare that they have no competing interests.

Funding

This work was supported by the Canadian Institutes of Health Research (CIHR) to J.T. (FND-148425). This work was also supported by a grant from the CIHR and Genome Canada (CEE-151619) to J.T. and Health Canada A-base funding to A.J.M. G.K. was supported by a Ferring Foundation Fellowship. J.T. is a Distinguished James McGill Professor. This research was enabled in part by support provided by Calcul Québec and the Digital Research Alliance of Canada.

Data availability

RRBS sequencing data is deposited at Gene Expression Ombinus (GEO) database accession number (GSE234855).

References

1. European IVF Monitoring Consortium (EIM), for the European Society of Human Reproduction and Embryology (ESHRE), Wyns C. *et al.* ART in Europe, 2018: results generated from European registries by ESHRE. *Hum Reprod Open* 2022;**2022**:hoac022.
2. Zhao J, Yan Y, Huang X. *et al.* Do the children born after assisted reproductive technology have an increased risk of birth defects? A systematic review and meta-analysis. *J Matern Fetal Neonatal Med* 2020;**33**:322–33.
3. DeBaun MR, Niemitz EL, Feinberg AP. Association of in vitro fertilization with Beckwith-Wiedemann syndrome and epigenetic alterations of LIT1 and H19. *Am J Hum Genet* 2003;**72**:156–60.
4. Ludwig M, Katalinic A, Gross S. *et al.* Increased prevalence of imprinting defects in patients with Angelman syndrome born to subfertile couples. *J Med Genet* 2005;**42**:289–91.
5. Hiura H, Okae H, Miyauchi N. *et al.* Characterization of DNA methylation errors in patients with imprinting disorders conceived by assisted reproduction technologies. *Hum Reprod* 2012;**27**:2541–8.
6. Hattori H, Hiura H, Kitamura A. *et al.* Association of four imprinting disorders and ART. *Clin Epigenetics* 2019;**11**:21.
7. White CR, MacDonald WA, Mann MR. Conservation of DNA methylation programming between mouse and human gametes and preimplantation embryos. *Biol Reprod* 2016;**95**:61.
8. Kindsfather AJ, Czekalski MA, Pressimone CA. *et al.* Perturbations in imprinted methylation from assisted reproductive technologies but not advanced maternal age in mouse preimplantation embryos. *Clin Epigenetics* 2019;**11**:162.
9. Fortier AL, Lopes FL, Darricarrere N. *et al.* Superovulation alters the expression of imprinted genes in the midgestation mouse placenta. *Hum Mol Genet* 2008;**17**:1653–65.
10. Market-Velker BA, Zhang L, Magri LS. *et al.* Dual effects of superovulation: loss of maternal and paternal imprinted methylation in a dose-dependent manner. *Hum Mol Genet* 2010;**19**:36–51.
11. Saenz-de-Juano MD, Billooye K, Smitz J. *et al.* The loss of imprinted DNA methylation in mouse blastocysts is inflicted to a similar extent by in vitro follicle culture and ovulation induction. *Mol Hum Reprod* 2016;**22**:427–41.
12. de Waal E, Vrooman LA, Fischer E. *et al.* The cumulative effect of assisted reproduction procedures on placental development and epigenetic perturbations in a mouse model. *Hum Mol Genet* 2015;**24**:6975–85.
13. de Waal E, Mak W, Calhoun S. *et al.* In vitro culture increases the frequency of stochastic epigenetic errors at imprinted genes in placental tissues from mouse concepti produced through assisted reproductive technologies. *Biol Reprod* 2014;**90**:22.
14. Rahimi S, Martel J, Karahan G. *et al.* Moderate maternal folic acid supplementation ameliorates adverse embryonic and epigenetic outcomes associated with assisted reproduction in a mouse model. *Hum Reprod* 2019;**34**:851–62.
15. Vrooman LA, Rhon-Calderon EA, Chao OY. *et al.* Assisted reproductive technologies induce temporally specific placental defects and the preeclampsia risk marker sFLT1 in mouse. *Development* 2020;**147**:dev186551.
16. Hwang SS, Dukhovny D, Gopal D. *et al.* Health of infants after ART-treated, subfertile, and fertile deliveries. *Pediatrics* 2018;**142**:e20174069.
17. Kobayashi H, Hiura H, John RM. *et al.* DNA methylation errors at imprinted loci after assisted conception originate in the parental sperm. *Eur J Hum Genet* 2009;**17**:1582–91.
18. Lambrot R, Xu C, Saint-Phar S. *et al.* Low paternal dietary folate alters the mouse sperm epigenome and is associated with negative pregnancy outcomes. *Nat Commun* 2013;**4**:2889.
19. Radford EJ, Ito M, Shi H. *et al.* In utero effects. In utero undernourishment perturbs the adult sperm methylome and intergenerational metabolism. *Science* 2014;**345**:1255903.
20. Donkin I, Versteyhe S, Ingerslev LR. *et al.* Obesity and bariatric surgery drive epigenetic variation of spermatozoa in humans. *Cell Metab* 2016;**23**:369–78.
21. Lismer A, Dumeaux V, Lafleur C. *et al.* Histone H3 lysine 4 trimethylation in sperm is transmitted to the embryo and associated with diet-induced phenotypes in the offspring. *Dev Cell* 2021;**56**:671–686.e6.
22. Pilsner JR, Shershebnev A, Wu H. *et al.* Aging-induced changes in sperm DNA methylation are modified by low dose of perinatal flame retardants. *Epigenomics* 2021;**13**:285–97.
23. Karahan G, Chan D, Shirane K. *et al.* Paternal MTHFR deficiency leads to hypomethylation of young retrotransposons and reproductive decline across two successive generations. *Development* 2021;**148**:dev199492.
24. Greenberg MVC, Bourc'his D. The diverse roles of DNA methylation in mammalian development and disease. *Nat Rev Mol Cell Biol* 2019;**20**:590–607.
25. Chedin F, Lieber MR, Hsieh CL. The DNA methyltransferase-like protein DNMT3L stimulates de novo methylation by Dnmt3a. *Proc Natl Acad Sci U S A* 2002;**99**:16916–21.
26. Neri F, Krepelova A, Incarnato D. *et al.* Dnmt3L antagonizes DNA methylation at bivalent promoters and favors DNA methylation at gene bodies in ESCs. *Cell* 2013;**155**:121–34.
27. Huang JX, Scott MB, Pu XY. *et al.* Association between single-nucleotide polymorphisms of DNMT3L and infertility with

azoospermia in Chinese men. *Reprod BioMed Online* 2012;**24**:66–71.
28. Montjean D, Ravel C, Benkhalifa M. *et al.* Methylation changes in mature sperm deoxyribonucleic acid from oligozoospermic men: assessment of genetic variants and assisted reproductive technology outcome. *Fertil Steril* 2013;**100**:1241–1247.e2.
29. Dong Y, Pan Y, Wang R. *et al.* Copy number variations in spermatogenic failure patients with chromosomal abnormalities and unexplained azoospermia. *Genet Mol Res* 2015;**14**:16041–9.
30. El-Maarri O, Kareta MS, Mikeska T. *et al.* A systematic search for DNA methyltransferase polymorphisms reveals a rare DNMT3L variant associated with subtelomeric hypomethylation. *Hum Mol Genet* 2009;**18**:1755–68.
31. Chen ZX, Mann JR, Hsieh CL. *et al.* Physical and functional interactions between the human DNMT3L protein and members of the de novo methyltransferase family. *J Cell Biochem* 2005;**95**:902–17.
32. Jia D, Jurkowska RZ, Zhang X. *et al.* Structure of Dnmt3a bound to Dnmt3L suggests a model for de novo DNA methylation. *Nature* 2007;**449**:248–51.
33. Bourc'his D, Xu GL, Lin CS. *et al.* Dnmt3L and the establishment of maternal genomic imprints. *Science* 2001;**294**:2536–9.
34. Bourc'his D, Bestor TH. Meiotic catastrophe and retrotransposon reactivation in male germ cells lacking Dnmt3L. *Nature* 2004;**431**:96–9.
35. Chong S, Vickaryous N, Ashe A. *et al.* Modifiers of epigenetic reprogramming show paternal effects in the mouse. *Nat Genet* 2007;**39**:614–22.
36. Zamudio N, Barau J, Teissandier A. *et al.* DNA methylation restrains transposons from adopting a chromatin signature permissive for meiotic recombination. *Genes Dev* 2015;**29**:1256–70.
37. Hales CM, Carroll MD, Fryar CD. *et al.* Prevalence of obesity and severe obesity among adults: United States, 2017–2018. *NCHS Data Brief* 2020;**360**:1–8.
38. Chambers TJ, Richard RA. The impact of obesity on male fertility. *Hormones (Athens)* 2015;**14**:563–8.
39. Keyhan S, Burke E, Schrott R. *et al.* Male obesity impacts DNA methylation reprogramming in sperm. *Clin Epigenetics* 2021;**13**:17.
40. de Castro Barbosa T, Ingerslev LR, Alm PS. *et al.* High-fat diet reprograms the epigenome of rat spermatozoa and transgenerationally affects metabolism of the offspring. *Mol Metab* 2016;**5**:184–97.
41. Wei Y, Yang CR, Wei YP. *et al.* Paternally induced transgenerational inheritance of susceptibility to diabetes in mammals. *Proc Natl Acad Sci U S A* 2014;**111**:1873–8.
42. Nguyen RH, Wilcox AJ, Skjaerven R. *et al.* Men's body mass index and infertility. *Hum Reprod* 2007;**22**:2488–93.
43. Mushtaq R, Pundir J, Achilli C. *et al.* Effect of male body mass index on assisted reproduction treatment outcome: an updated systematic review and meta-analysis. *Reprod BioMed Online* 2018;**36**:459–71.
44. Kaati G, Bygren LO, Edvinsson S. Cardiovascular and diabetes mortality determined by nutrition during parents' and grandparents' slow growth period. *Eur J Hum Genet* 2002;**10**:682–8.
45. Pembrey ME, Bygren LO, Kaati G. *et al.* Sex-specific, male-line transgenerational responses in humans. *Eur J Hum Genet* 2006;**14**:159–66.
46. Ng SF, Lin RC, Laybutt DR. *et al.* Chronic high-fat diet in fathers programs β-cell dysfunction in female rat offspring. *Nature* 2010;**467**:963–6.
47. Fullston T, Palmer NO, Owens JA. *et al.* Diet-induced paternal obesity in the absence of diabetes diminishes the reproductive health of two subsequent generations of mice. *Hum Reprod* 2012;**27**:1391–400.
48. Fullston T, Ohlsson Teague EM, Palmer NO. *et al.* Paternal obesity initiates metabolic disturbances in two generations of mice with incomplete penetrance to the F2 generation and alters the transcriptional profile of testis and sperm microRNA content. *FASEB J* 2013;**27**:4226–43.
49. Yoshimizu T, Sugiyama N, De Felice M. *et al.* Germline-specific expression of the Oct-4/green fluorescent protein (GFP) transgene in mice. *Develop Growth Differ* 1999;**41**:675–84.
50. Rabot S, Membrez M, Blancher F. *et al.* High fat diet drives obesity regardless the composition of gut microbiota in mice. *Sci Rep* 2016;**6**:32484.
51. Pepin AS, Lafleur C, Lambrot R. *et al.* Sperm histone H3 lysine 4 tri-methylation serves as a metabolic sensor of paternal obesity and is associated with the inheritance of metabolic dysfunction. *Mol Metab* 2022;**59**:101463.
52. Niles KM, Yeh JR, Chan D. *et al.* Haploinsufficiency of the paternal-effect gene Dnmt3L results in transient DNA hypomethylation in progenitor cells of the male germline. *Hum Reprod* 2013;**28**:519–30.
53. Gu H, Smith ZD, Bock C. *et al.* Preparation of reduced representation bisulfite sequencing libraries for genome-scale DNA methylation profiling. *Nat Protoc* 2011;**6**:468–81.
54. Boyle P, Clement K, Gu H. *et al.* Gel-free multiplexed reduced representation bisulfite sequencing for large-scale DNA methylation profiling. *Genome Biol* 2012;**13**:R92.
55. McGraw S, Zhang JX, Farag M. *et al.* Transient DNMT1 suppression reveals hidden heritable marks in the genome. *Nucleic Acids Res* 2015;**43**:1485–97.
56. Legault LM, Chan D, McGraw S. Rapid multiplexed reduced representation bisulfite sequencing library prep (rRRBS). *Bio Protoc* 2019;**9**:e3171.
57. Xi Y, Li W. BSMAP: whole genome bisulfite sequence MAPping program. *BMC Bioinformatics* 2009;**10**:232.
58. Akalin A, Kormaksson M, Li S. *et al.* methylKit: a comprehensive R package for the analysis of genome-wide DNA methylation profiles. *Genome Biol* 2012;**13**:R87.
59. Heinz S, Benner C, Spann N. *et al.* Simple combinations of lineage-determining transcription factors prime cis-regulatory elements required for macrophage and B cell identities. *Mol Cell* 2010;**38**:576–89.
60. Liao Y, Wang J, Jaehnig EJ. *et al.* WebGestalt 2019: gene set analysis toolkit with revamped UIs and APIs. *Nucleic Acids Res* 2019;**47**:W199–205.
61. Smit AFA, Hubley R, Green P. *RepeatMasker Open-4.0* 2013–2015; accessed in May 2022. http://www.repeatmasker.org.
62. Ihirwe RG, Martel J, Rahimi S. *et al.* Protective and sex-specific effects of moderate dose folic acid supplementation on the placenta following assisted reproduction in mice. *FASEB J* 2023;**37**:e22677.
63. Bensadoun A, Weinstein D. Assay of proteins in the presence of interfering materials. *Anal Biochem* 1976;**70**:241–50.
64. Byers SL, Payson SJ, Taft RA. Performance of ten inbred mouse strains following assisted reproductive technologies (ARTs). *Theriogenology* 2006;**65**:1716–26.
65. Behringer R, Gertsenstein M, Nagy KV. *et al. Manipulating the Mouse Embryo: a Laboratory Manual*, 2014.
66. Whidden L, Martel J, Rahimi S. *et al.* Compromised oocyte quality and assisted reproduction contribute to sex-specific effects on offspring outcomes and epigenetic patterning. *Hum Mol Genet* 2016;**25**:4649–60.

67. Gagnier L, Belancio VP, Mager DL. Mouse germ line mutations due to retrotransposon insertions. *Mob DNA* 2019;**10**:15.
68. Schauer SN, Carreira PE, Shukla R. *et al.* L1 retrotransposition is a common feature of mammalian hepatocarcinogenesis. *Genome Res* 2018;**28**:639–53.
69. Kose S, Sozlu S, Bolukbasi H. *et al.* Obesity is associated with folate metabolism. *Int J Vitam Nutr Res* 2020;**90**:353–64.
70. Reig A, Seli E. The association between assisted reproductive technologies and low birth weight. *Curr Opin Obstet Gynecol* 2019;**31**:183–7.
71. Bloise E, Lin W, Liu X. *et al.* Impaired placental nutrient transport in mice generated by in vitro fertilization. *Endocrinology* 2012;**153**:3457–67.
72. Mann MR, Lee SS, Doherty AS. *et al.* Selective loss of imprinting in the placenta following preimplantation development in culture. *Development* 2004;**131**:3727–35.
73. Chooi YC, Ding C, Magkos F. The epidemiology of obesity. *Metabolism* 2019;**92**:6–10.
74. Li J, Tsuprykov O, Yang X. *et al.* Paternal programming of offspring cardiometabolic diseases in later life. *J Hypertens* 2016;**34**:2111–26.
75. Carone BR, Fauquier L, Habib N. *et al.* Paternally induced transgenerational environmental reprogramming of metabolic gene expression in mammals. *Cell* 2010;**143**:1084–96.
76. Grandjean V, Fourre S, De Abreu DA. *et al.* RNA-mediated paternal heredity of diet-induced obesity and metabolic disorders. *Sci Rep* 2015;**5**:18193.
77. La Salle S, Mertineit C, Taketo T. *et al.* Windows for sex-specific methylation marked by DNA methyltransferase expression profiles in mouse germ cells. *Dev Biol* 2004;**268**:403–15.
78. Zamudio NM, Scott HS, Wolski K. *et al.* DNMT3L is a regulator of X chromosome compaction and post-meiotic gene transcription. *PLoS One* 2011;**6**:e18276.
79. Gong M, Dong W, He T. *et al.* MTHFR 677C>T polymorphism increases the male infertility risk: a meta-analysis involving 26 studies. *PLoS One* 2015;**10**:e0121147.
80. Garner JL, Niles KM, McGraw S. *et al.* Stability of DNA methylation patterns in mouse spermatogonia under conditions of MTHFR deficiency and methionine supplementation. *Biol Reprod* 2013;**89**:125.
81. Zymperdikas CF, Zymperdikas VF, Mastorakos G. *et al.* Assisted reproduction technology outcomes in women with infertility and preexisting diabetes mellitus: a systematic review. *Hormones (Athens)* 2022;**21**:23–31.
82. Sha T, Wang X, Cheng W. *et al.* A meta-analysis of pregnancy-related outcomes and complications in women with polycystic ovary syndrome undergoing IVF. *Reprod BioMed Online* 2019;**39**:281–93.
83. Choufani S, Turinsky AL, Melamed N. *et al.* Impact of assisted reproduction, infertility, sex and paternal factors on the placental DNA methylome. *Hum Mol Genet* 2019;**28**:372–85.
84. Roach AN, Zimmel KN, Thomas KN. *et al.* Preconception paternal alcohol exposure decreases IVF embryo survival and pregnancy success rates in a mouse model. *Mol Hum Reprod* 2023;**29**:gaad002.
85. Denomme MM, Parks JC, McCallie BR. *et al.* Advanced paternal age directly impacts mouse embryonic placental imprinting. *PLoS One* 2020;**15**:e0229904.
86. Marshall KL, Rivera RM. The effects of superovulation and reproductive aging on the epigenome of the oocyte and embryo. *Mol Reprod Dev* 2018;**85**:90–105.
87. Market-Velker BA, Fernandes AD, Mann MR. Side-by-side comparison of five commercial media systems in a mouse model: suboptimal in vitro culture interferes with imprint maintenance. *Biol Reprod* 2010;**83**:938–50.
88. Market Velker BA, Denomme MM, Mann MR. Loss of genomic imprinting in mouse embryos with fast rates of preimplantation development in culture. *Biol Reprod* 2012;**86**:143.
89. Ducreux B, Barberet J, Guilleman M. *et al.* Assessing the influence of distinct culture media on human pre-implantation development using single-embryo transcriptomics. *Front Cell Dev Biol* 2023;**11**:1155634.
90. Carmignac V, Barberet J, Iranzo J. *et al.* Effects of assisted reproductive technologies on transposon regulation in the mouse preimplanted embryo. *Hum Reprod* 2019;**34**:612–22.
91. Vrooman LA, Rhon-Calderon EA, Suri KV. *et al.* Placental abnormalities are associated with specific windows of embryo culture in a mouse model. *Front Cell Dev Biol* 2022;**10**:884088.
92. Jachowicz JW, Bing X, Pontabry J. *et al.* LINE-1 activation after fertilization regulates global chromatin accessibility in the early mouse embryo. *Nat Genet* 2017;**49**:1502–10.
93. Han LJ, He XF, Ye XH. Methylenetetrahydrofolate reductase C677T and A1298C polymorphisms and male infertility risk: an updated meta-analysis. *Medicine (Baltimore)* 2020;**99**:e23662.
94. Chan D, Shao X, Dumargne MC. *et al.* Customized MethylC-capture sequencing to evaluate variation in the human sperm DNA methylome representative of altered folate metabolism. *Environ Health Perspect* 2019;**127**:87002.
95. Poorang S, Abdollahi S, Anvar Z. *et al.* The impact of methylenetetrahydrofolate reductase (MTHFR) sperm methylation and variants on semen parameters and the chance of recurrent pregnancy loss in the couple. *Clin Lab* 2018;**64**:1121–8.
96. Liu Y, Zhang F, Dai L. C677T polymorphism increases the risk of early spontaneous abortion. *J Assist Reprod Genet* 2019;**36**:1737–41.